

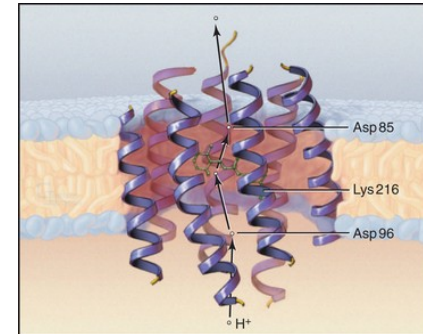
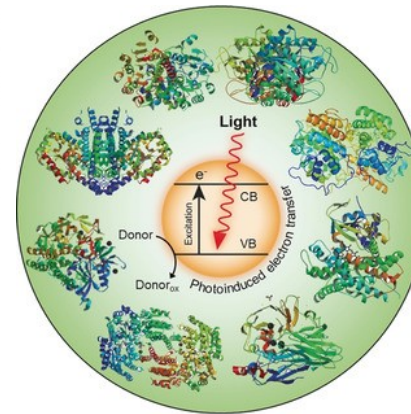
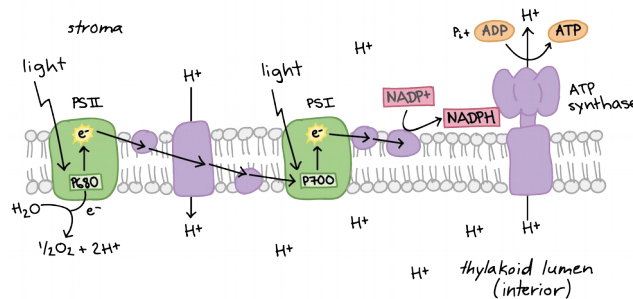
Multiscale modeling of charge transfer reactions in biological systems

Laura Zanetti Polzi

Charge Transfer in Biological Systems

“Life on earth is energized by the stepwise vectorial transport of individual electrons and protons.”*

- Photosynthesis
- Respiration
- Proton pumping
- Catalysis
- ...



Hybrid quantum/classical approaches

- Proper treatment of the reaction event at the quantum level
- Proper description of the complexity of the system
- Interplay between reactants and environment considered



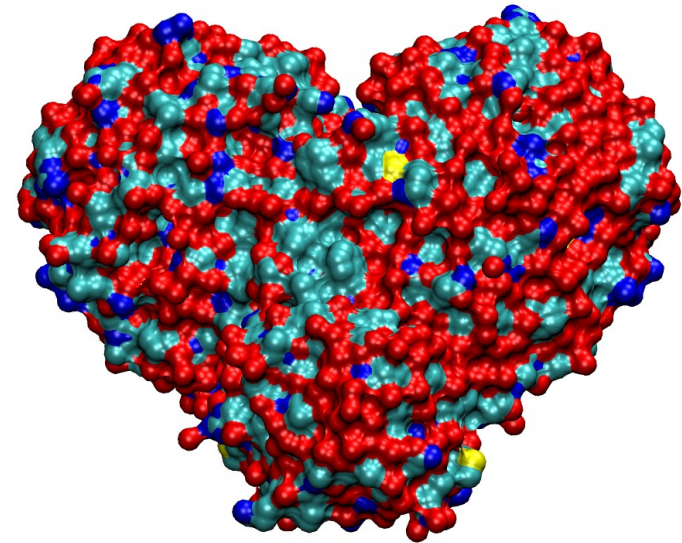
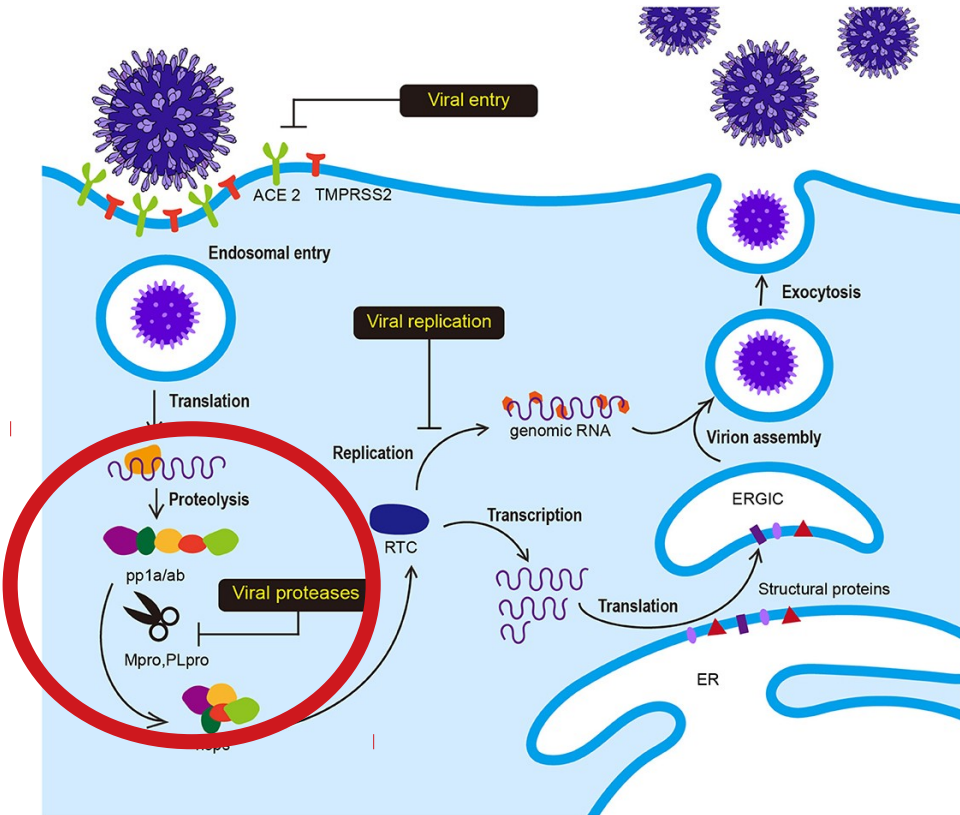
Interpretation at the molecular level of the reaction/process of interest

Two charge transfer reactions

- The catalytic proton transfer (PT) reaction in SARS-CoV-2 main protease (Mpro)
- The light-induced electron transfer (ET) reaction in lactate monooxygenase (LMO)

SARS-Cov-2 main protease (Mpro)

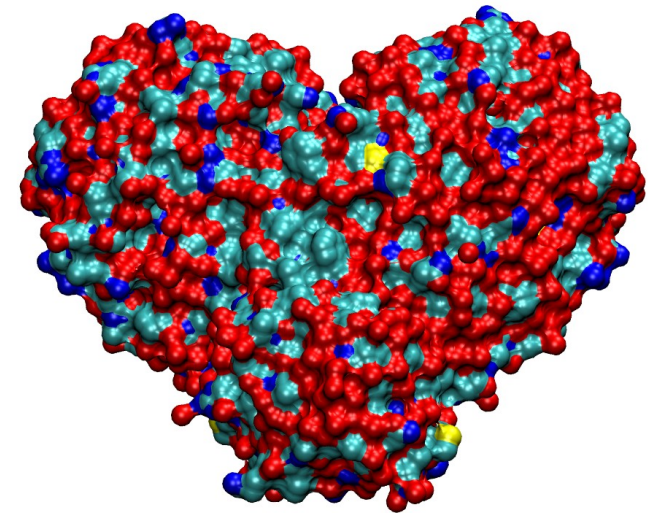
Mpro plays a key role in viral replication and transcription



SARS-Cov-2 main protease (Mpro)

Mpro is one of the most promising targets for drug development

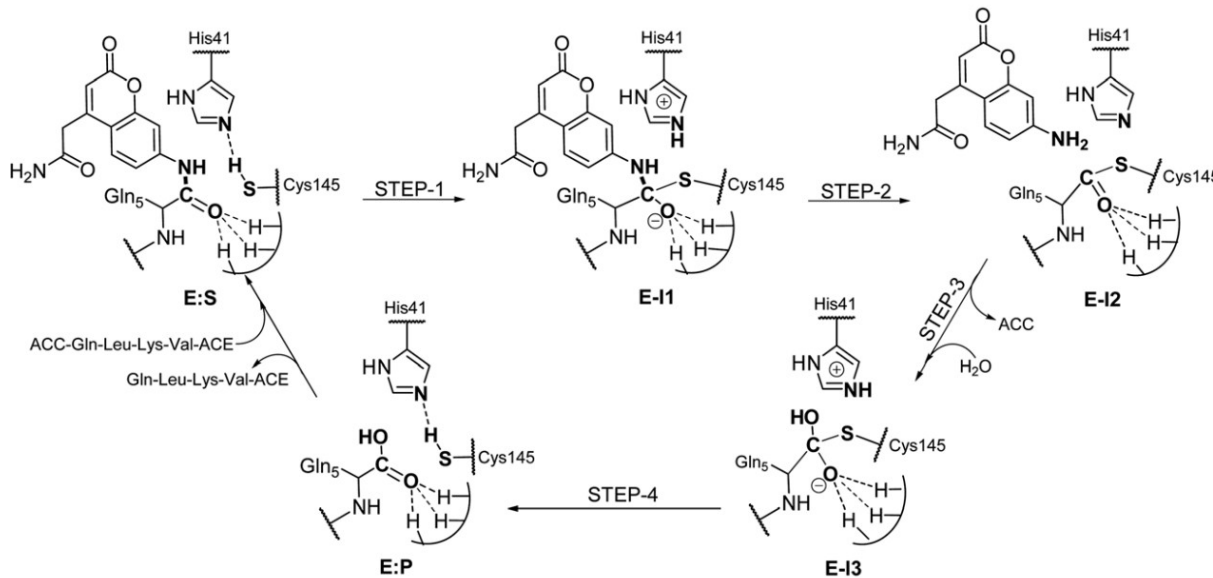
- Inhibition of its cleaving activity would block the viral replication cycle
- Its recognition sequence is different from that of all human proteases
- Mpro structure is very similar among the coronaviruses family



SARS-Cov-2 main protease (Mpro)

Cysteine-histidine catalytic dyad (Cys145/His41)

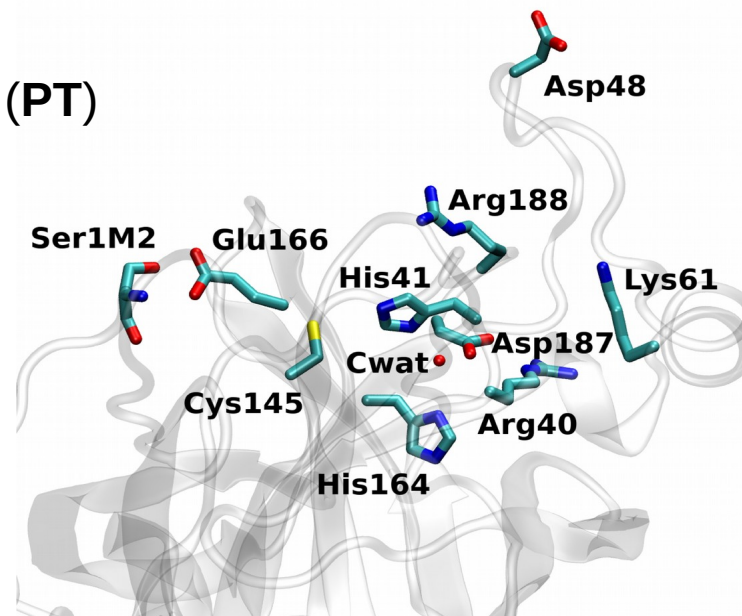
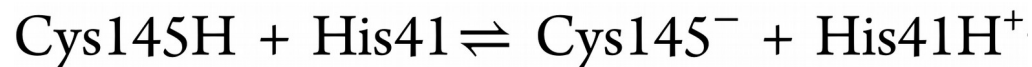
Protein hydrolysis mediated by Cys145 that binds to the carbonyl carbon of a susceptible peptide bond



SARS-Cov-2 main protease (Mpro)

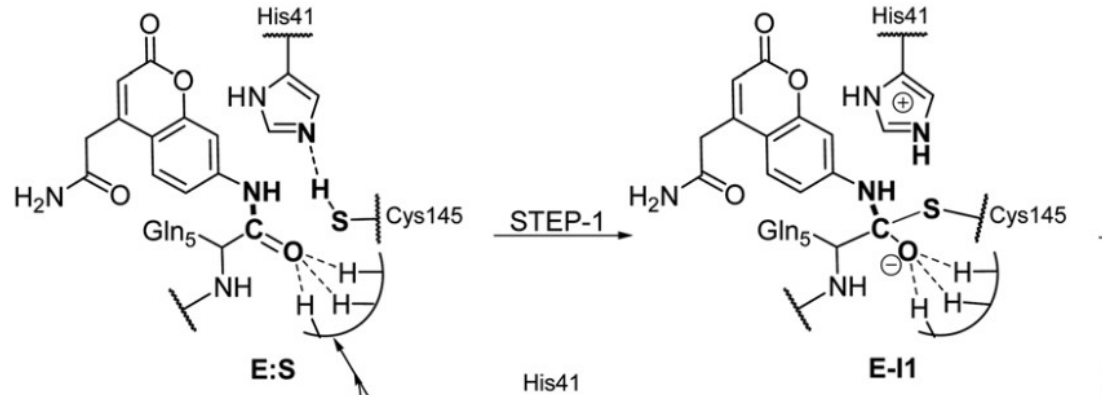
Cysteine-histidine catalytic dyad (Cys145/His41)

The imidazole of **His41** is the base of the proton transfer (PT) reaction leading to a highly reactive zwitterionic couple:



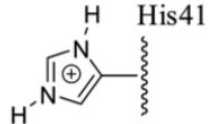
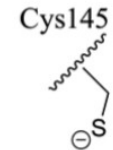
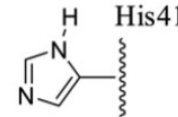
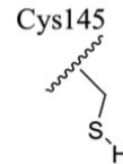
SARS-Cov-2 main protease (Mpro)

- The covalent binding of some classes of inhibitors (such as Michael acceptors and ketoamides) also requires **deprotonated Cys145** through a **PT** to **His41**.



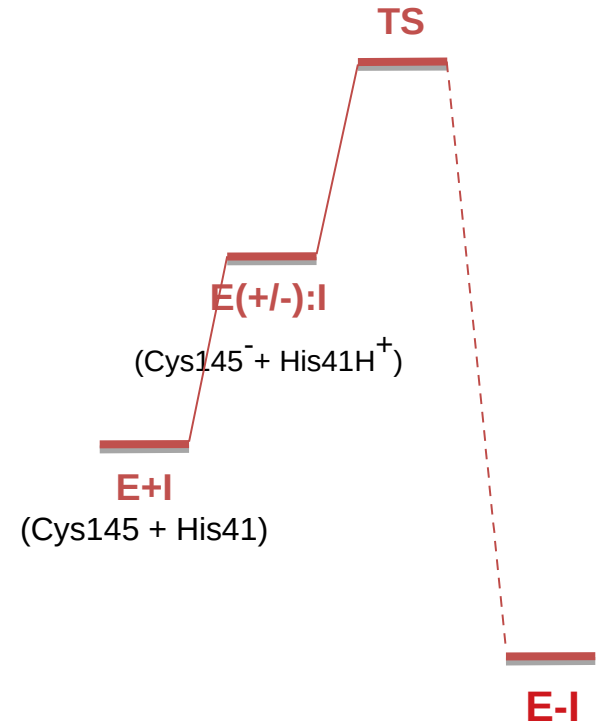
SARS-Cov-2 main protease (Mpro)

- The covalent binding of some classes of inhibitors (such as Michael acceptors and ketoamides) also requires **deprotonated Cys145** through a **PT** to **His41**.
- The inability to efficiently promote the **PT** reaction has been suggested to determine the low inhibition potencies of some known inhibitors*.



SARS-Cov-2 main protease (Mpro)

- The covalent binding of some classes of inhibitors (such as Michael acceptors and ketoamides) also requires **deprotonated Cys145** through a **PT** to **His41**.
- The inability to efficiently promote the **PT** reaction has been suggested to determine the low inhibition potencies of some known inhibitors*.
- The PT reaction free energy in the presence of two inhibitors (**N3** and α -ketoamide **13b**) accounts for **40-50%** of the total activation free energy for the formation of the covalent complex**.

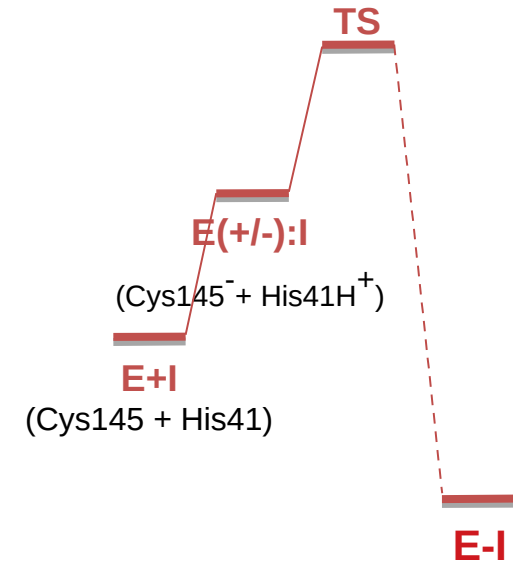


SARS-Cov-2 main protease (Mpro)



The improvement of the stability of the charged catalytic dyad by the inhibitor binding could be a strategy to promote inhibition

Knowledge of the protein regions capable of affecting the **PT** reaction is a crucial point for the design and screening of potential inhibitors



SARS-Cov-2 main protease (Mpro)

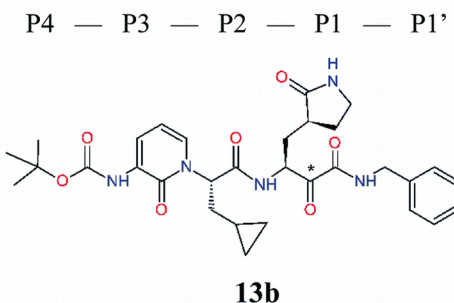
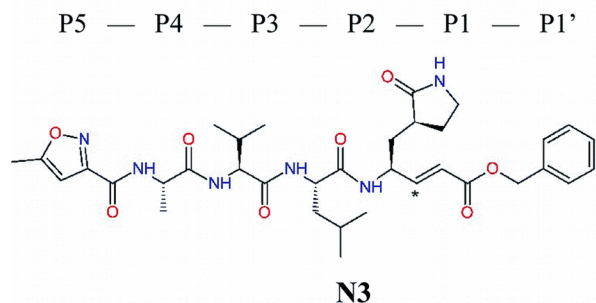


Here we focus on the investigation of the thermodynamics of the PT reaction in the apo enzyme and in complex with two inhibitors

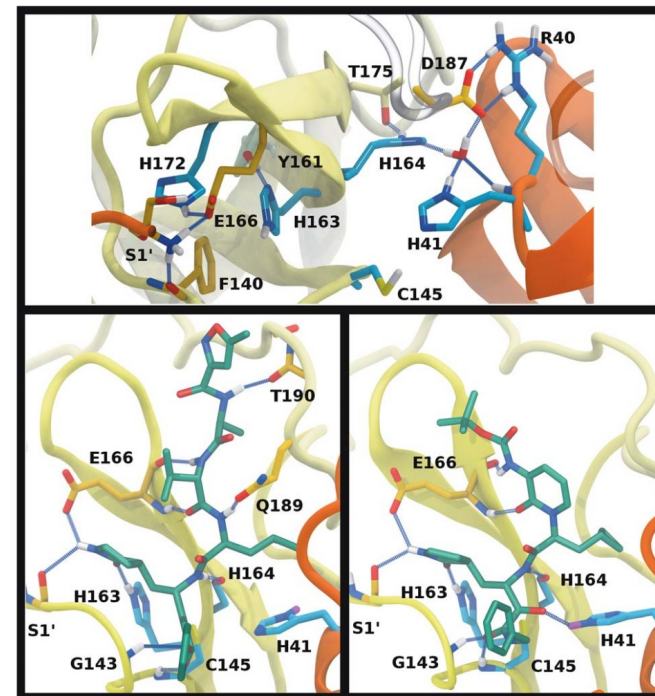
The main aim is to identify the enzyme regions and specific water molecules that control the activation of the catalytic **PT reaction**

Protonation state of key residues

MD simulations to investigate the effects of different protonation states for crucial residues in Mpro in both the **apo** form as well as **ligand-bound complexes**

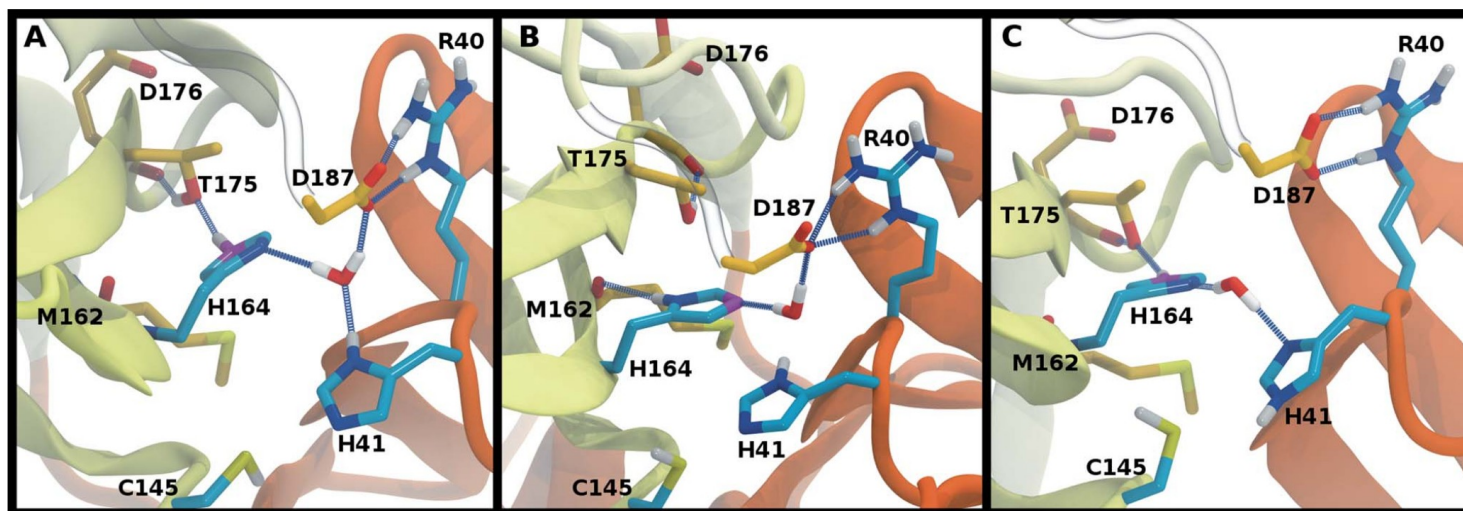


Peptidomimetic covalent inhibitors **N3** and **13b**



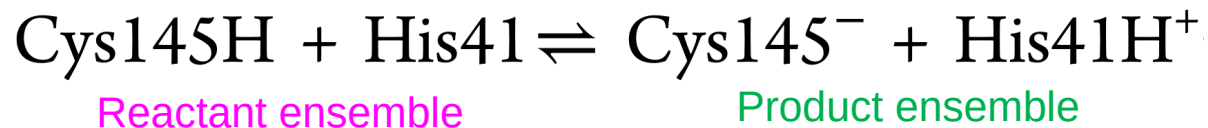
Protonation state of key residues

The combination of protonation states for histidines in or near the catalytic site can have a profound impact on Mpro's structural stability



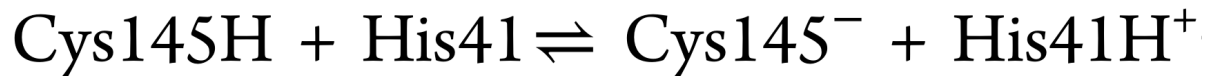
Modelling the PT reaction

We treat at the QM level a small portion of the system (the **QC**, here **Cys/His sidechains**) while the rest of the system (the **environment**) exerts a **classical electrostatic perturbation** on the **QC***



MD simulations* of the **apo** enzyme: in the reactant ensemble and in the product ensemble

Modelling the PT reaction



Reactant ensemble

Product ensemble

QM calculations of gas-phase electronic Hamiltonian eigenstates for the quantum centers (QCs):

⇒ Unperturbed energies and dipoles for C/H

⇒ Unperturbed energies and dipoles for C-/H+

$$H_{\text{QC}}^{\circ} = \begin{pmatrix} E_{S0,\text{QC}}^{\circ} & 0 & 0 & \dots \\ 0 & E_{S1,\text{QC}}^{\circ} & 0 & \dots \\ 0 & 0 & E_{S2,\text{QC}}^{\circ} & \dots \\ & \vdots & & \ddots \end{pmatrix}$$

Modelling the PT reaction

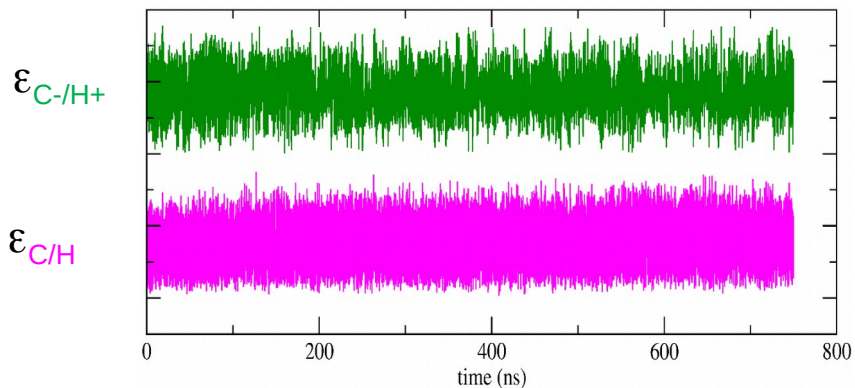
Construction and **diagonalization** of the perturbed Hamiltonian matrix in order to get the **perturbed** energies at each step of the **MD simulation**:

$$V_{i,j} = q_{qc} \mathcal{V}(r_0) - \mathbf{E}(r_0) \cdot \langle \Phi_i^0 | \hat{\boldsymbol{\mu}}_{i,j} | \Phi_j^0 \rangle$$

environment electrostatic potential \nearrow \nwarrow environment electric field

$$H_{QC}^P = \begin{pmatrix} E_{S0,QC}^{\circ} + V_{00,QC} & V_{01} & V_{02} & \dots & \dots \\ V_{10} & E_{S1,QC}^{\circ} + V_{11} & V_{12} & \dots & \dots \\ V_{20} & V_{21} & E_{S2,QC}^{\circ} + V_{22} & \dots & \dots \\ \vdots & \vdots & \vdots & \ddots & \ddots \end{pmatrix}$$

Instantaneous perturbed eigevalues

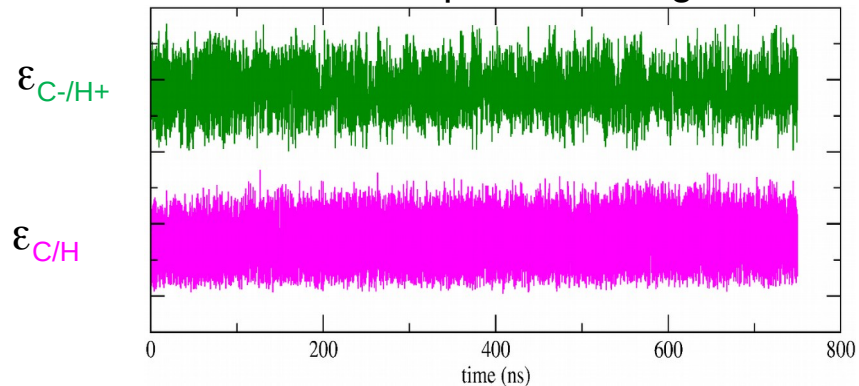


Product ensemble $\text{Cys145}^- + \text{His41H}^+$

Reactant ensemble $\text{Cys145H} + \text{His41}$

Modelling the PT reaction

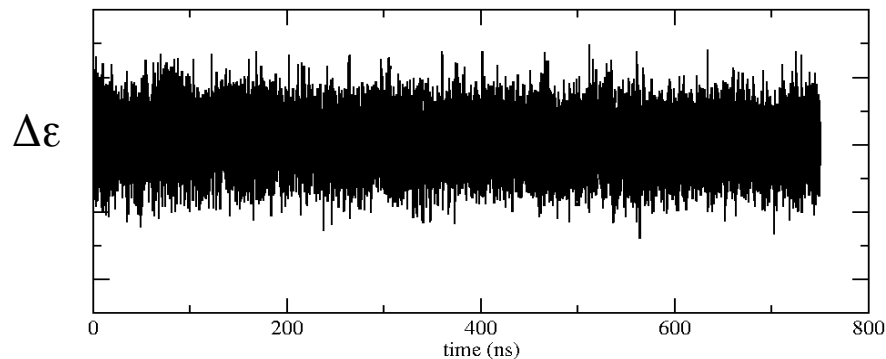
Instantaneous perturbed eigenvalues



Product ensemble Cys145⁻ + His41H⁺

Reactant ensemble Cys145H + His41:

Calculation of the PT energy variation



$$\Delta\varepsilon = \varepsilon_{C-/H+} - \varepsilon_{C/H}$$

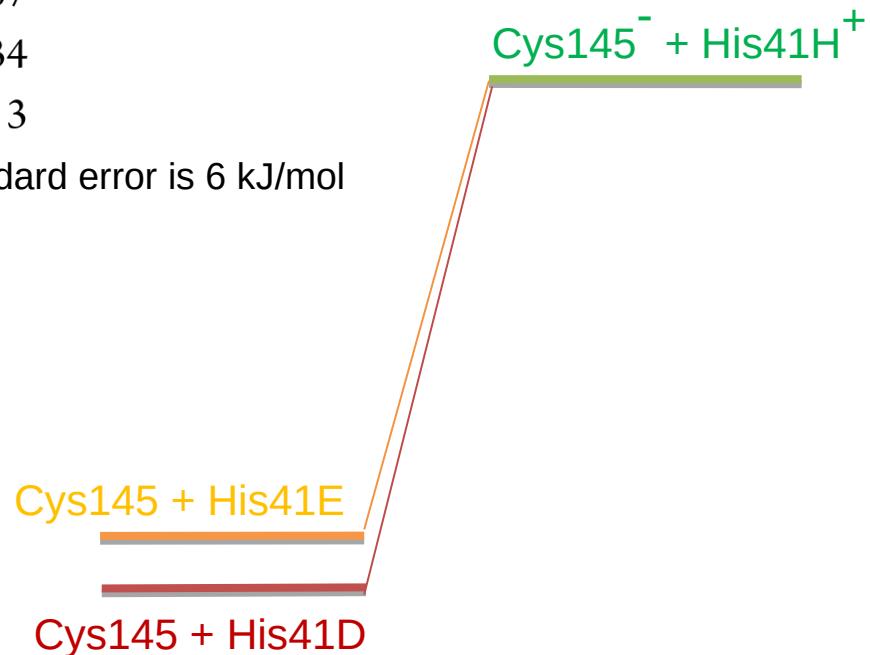
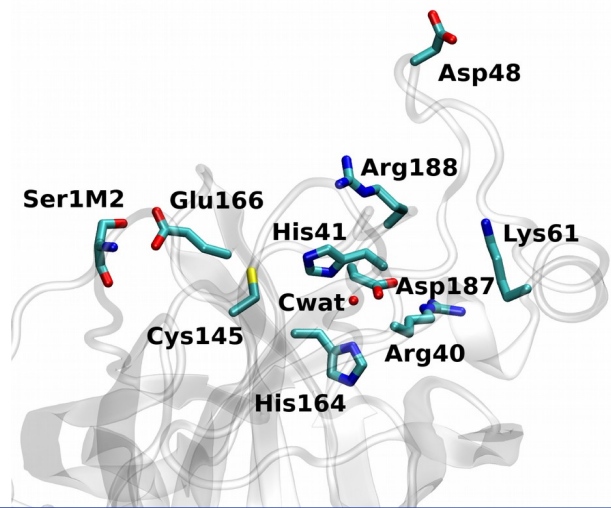
Calculation of the free energy change, ΔG° , from the $\Delta\varepsilon$:

$$\Delta G^\circ \cong \frac{k_B T}{2} \ln \frac{\langle e^{\beta \Delta\varepsilon} \rangle_P}{\langle e^{-\beta \Delta\varepsilon} \rangle_R}$$

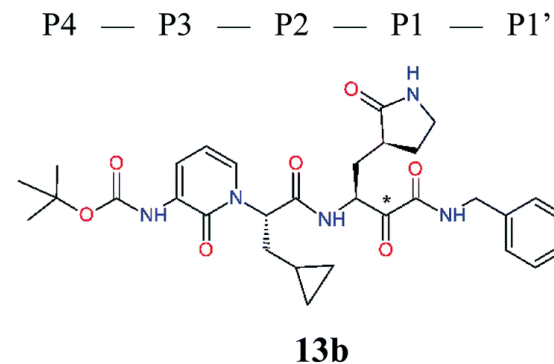
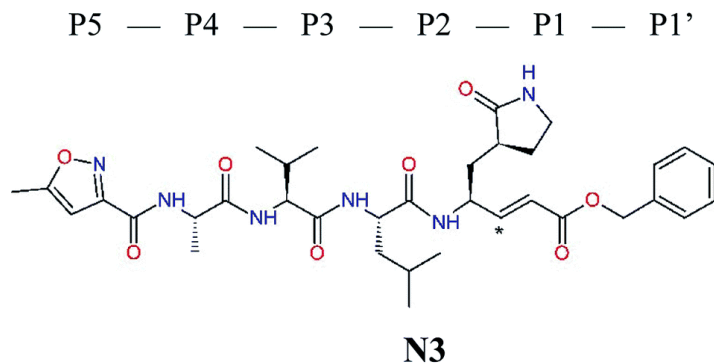
PT reaction in the apo state

	ΔG^0 *
$(\text{Cys145H} + \text{His41E} \rightleftharpoons \text{Cys145}^- + \text{His41H}^+)_{\text{apo}}$	37
$(\text{Cys145H} + \text{His41D} \rightleftharpoons \text{Cys145}^- + \text{His41H}^+)_{\text{apo}}$	34
$(\text{His41E} \rightleftharpoons \text{His41D})_{\text{apo}}$	3

*kJ/mol, mean standard error is 6 kJ/mol



PT reaction with inhibitors



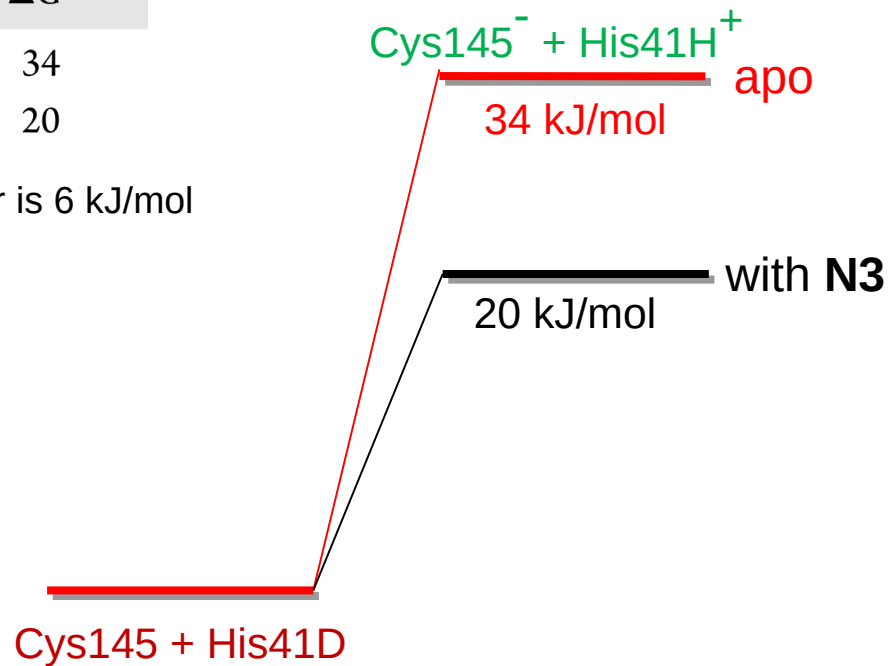
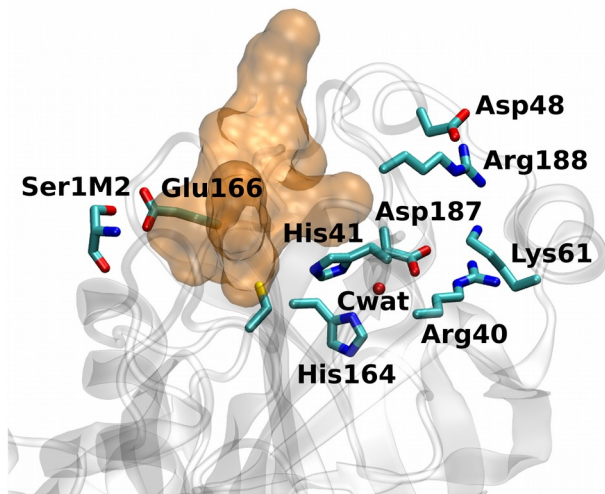
Peptidomimetic covalent inhibitors **N3** and **13b**

Stars (*) indicate the sites of nucleophilic attack of anionic sulphur of cysteine of the catalytic dyad

PT reaction with inhibitor N3

	ΔG^0	*
$(\text{Cys145H} + \text{His41D} \rightleftharpoons \text{Cys145}^- + \text{His41H}^+)_{\text{apo}}$	34	
$(\text{Cys145H} + \text{His41D} \rightleftharpoons \text{Cys145}^- + \text{His41H}^+)_{\text{N3}}$	20	

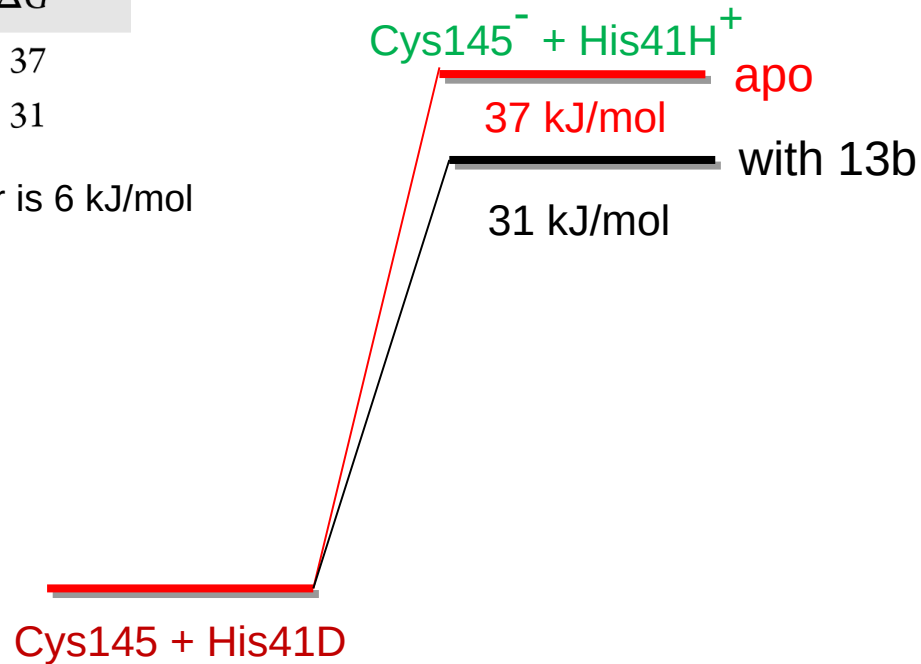
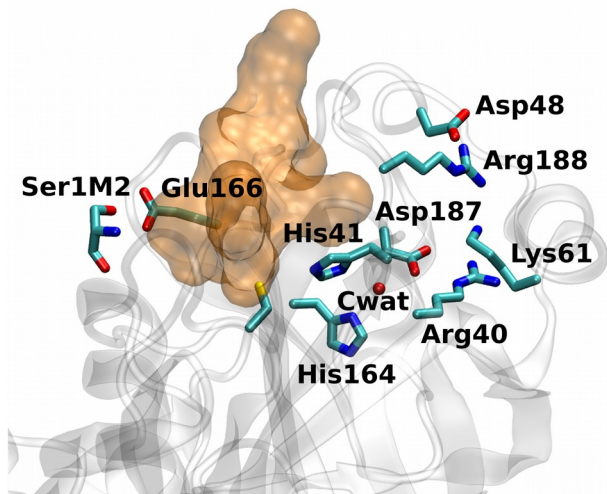
*kJ/mol, mean standard error is 6 kJ/mol



PT reaction with inhibitor 13b

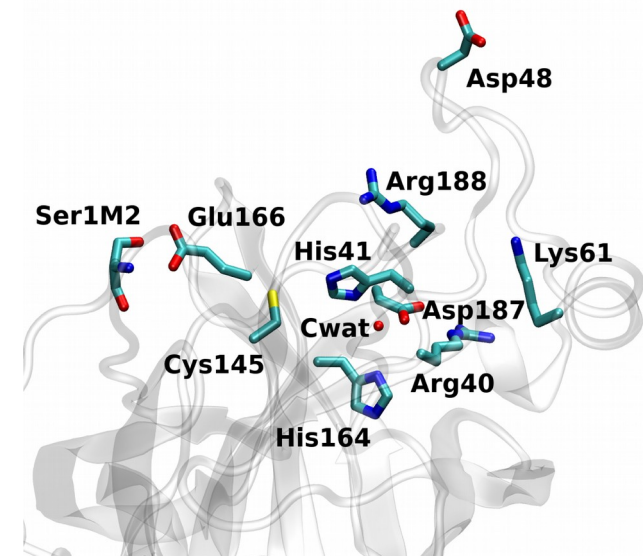
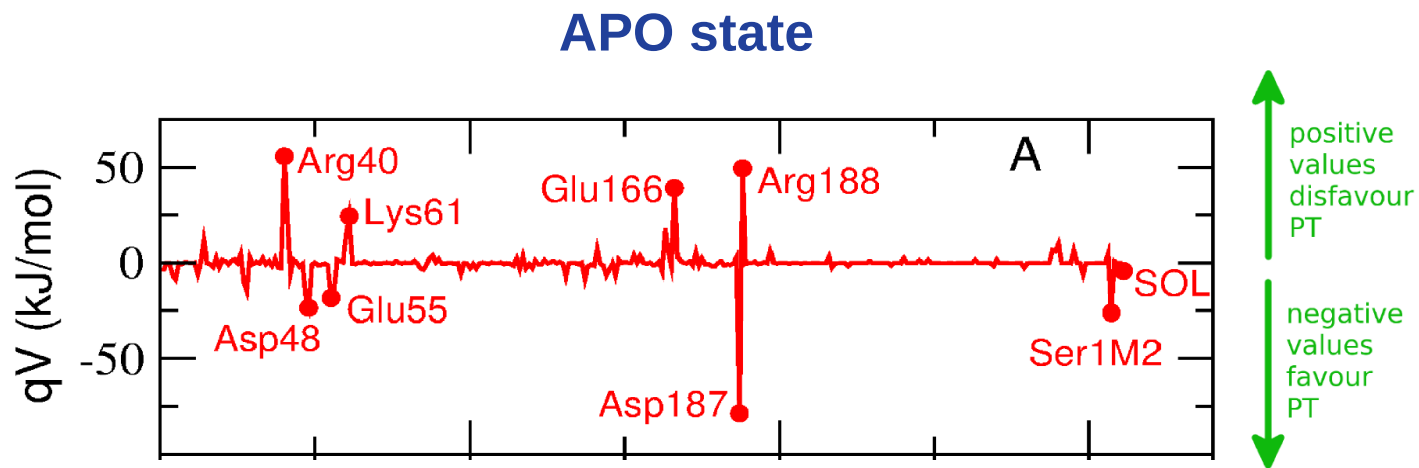
	ΔG^0	*
$(\text{Cys145H} + \text{His41E} \rightleftharpoons \text{Cys145}^- + \text{His41H}^+)_{\text{apo}}$	37	
$(\text{Cys145H} + \text{His41E} \rightleftharpoons \text{Cys145}^- + \text{His41H}^+)_{13\text{b}}$	31	

*kJ/mol, mean standard error is 6 kJ/mol



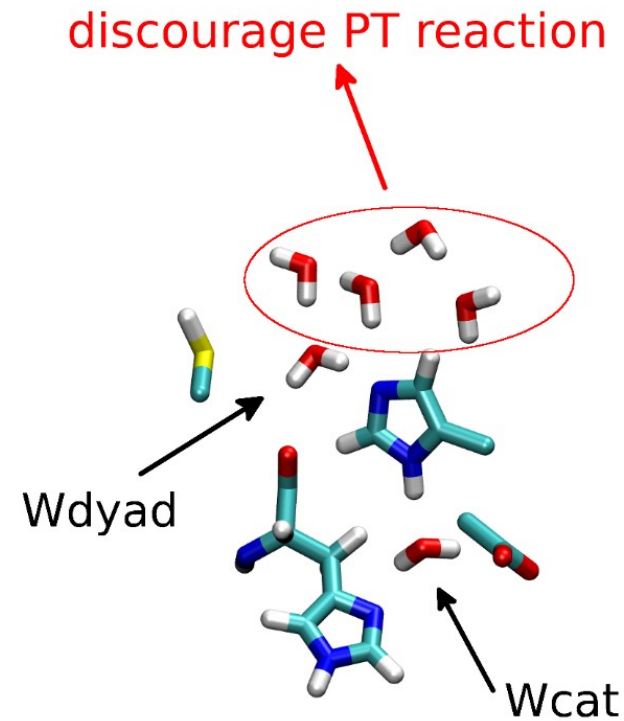
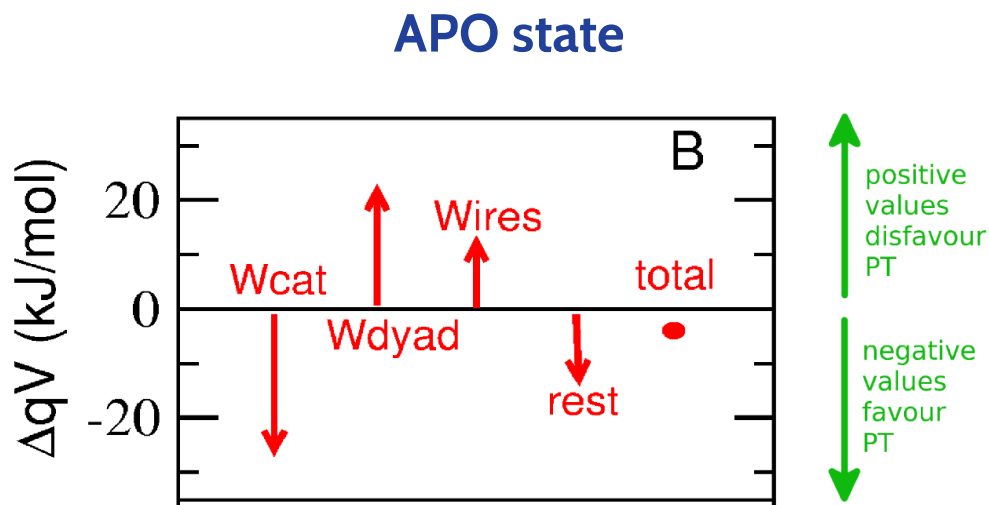
Molecular contributions to the PT energetics

Analysis of the contribution of each protein residue to the **electrostatic potential** to understand which protein regions contribute the most to the **PT** energy

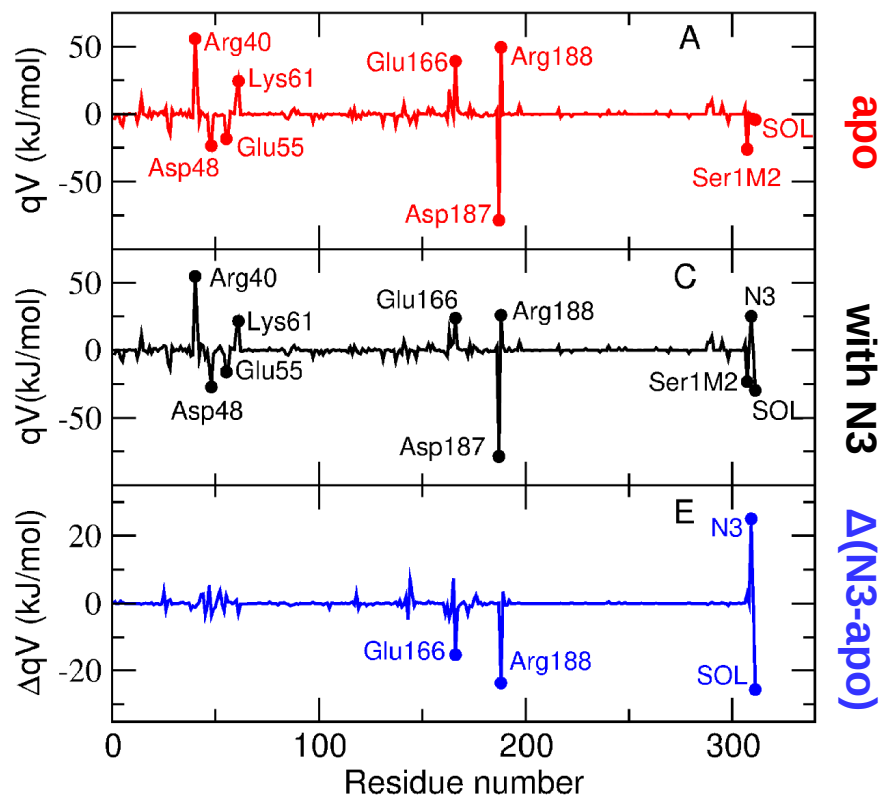


Molecular contributions to the PT energetics

Analysis of the contribution of each protein residue to the **electrostatic potential** to understand which protein regions contribute the most to the **PT** energy



Molecular contributions to the PT energetics

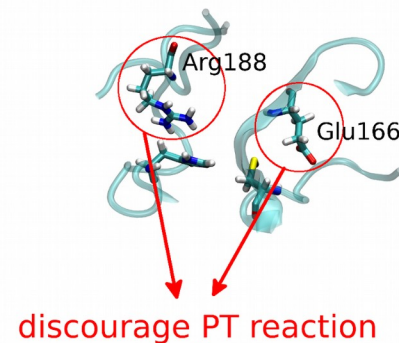


apo

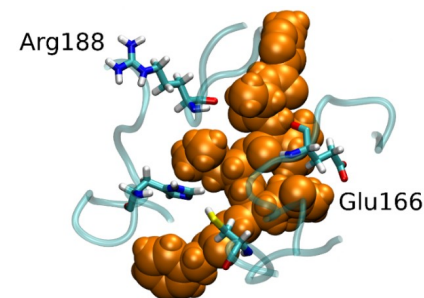
with N3

$\Delta(N3-apo)$

positive values disfavour PT
negative values favour PT

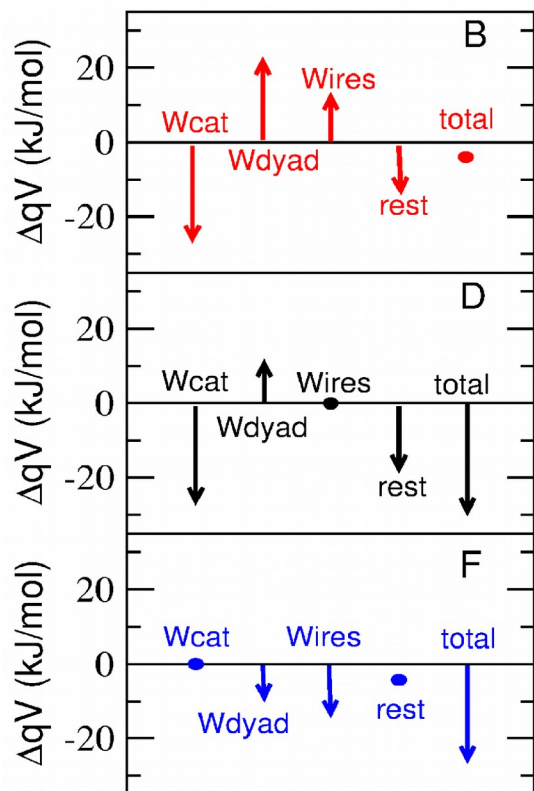


APO state



with N3

Molecular contributions to the PT energetics

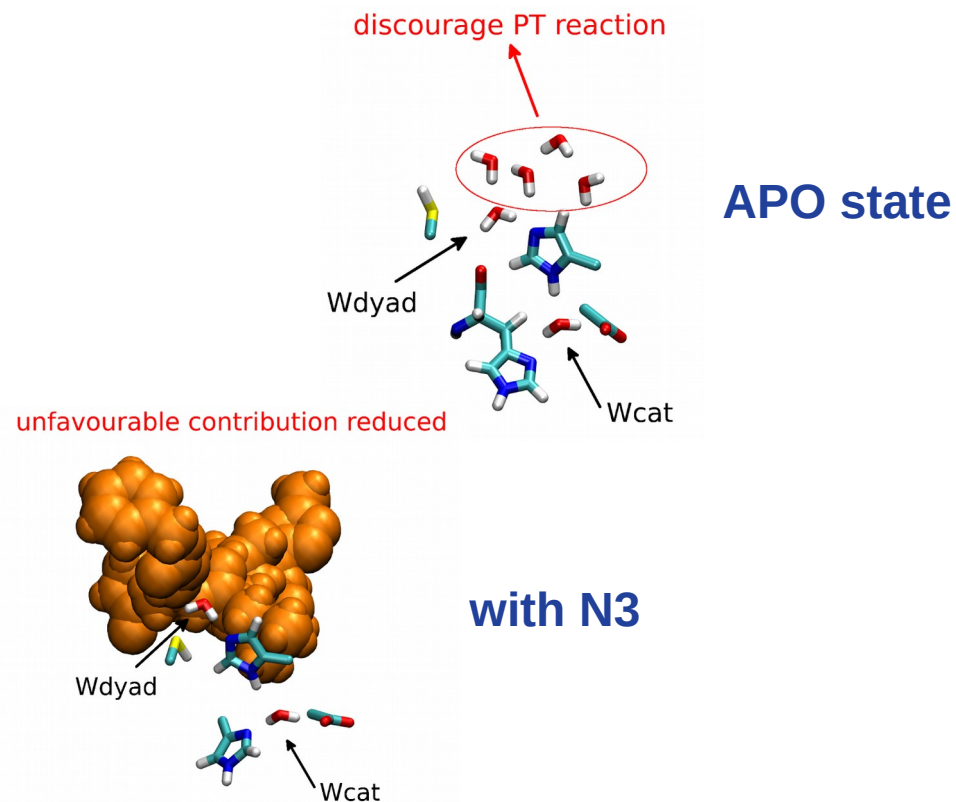


apo

with N3

$\Delta(N3-apo)$

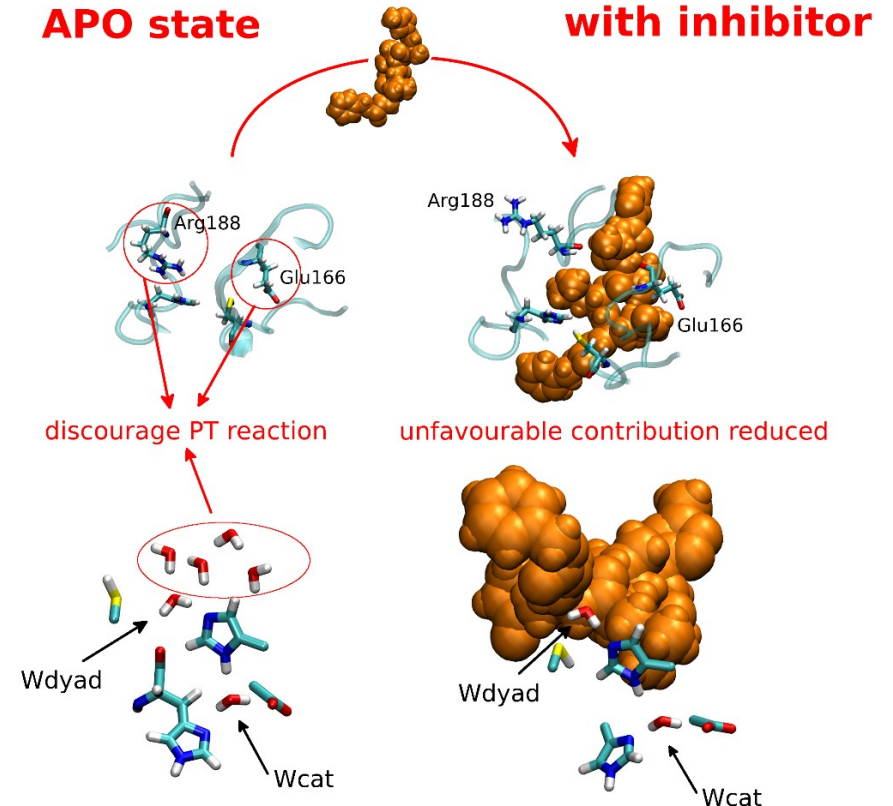
positive values disfavour PT
negative values favour PT



In Summary

The present results can help identify:

- **compounds** that can **promote** the catalytic **PT reaction** and, therefore, be good candidates as covalent inhibitors;
- specific **water molecules** able to affect the PT energetics and that could be explicitly included in docking procedures;
- **key sites** that can be targeted with ligands, in the framework of **allosteric inhibition**, to suppress the enzymatic activity.



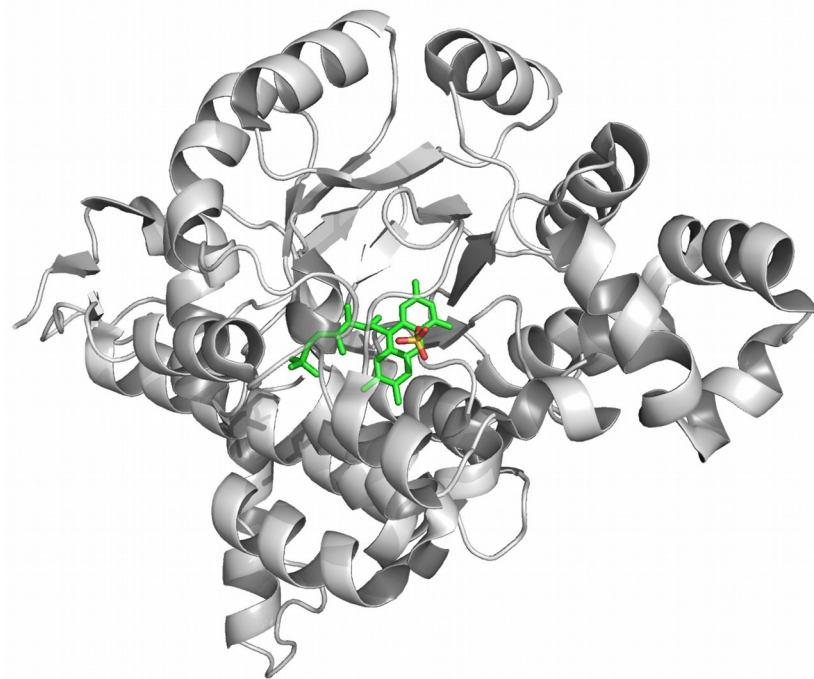
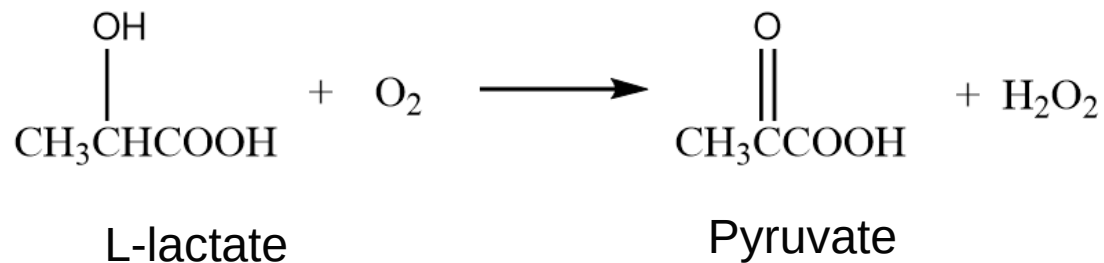
Two charge transfer reactions

- The catalytic proton transfer (PT) reaction in SARS-CoV-2 main protease (Mpro)
- The light-induced electron transfer (ET) reaction in lactate monooxygenase (LMO)

An ongoing work

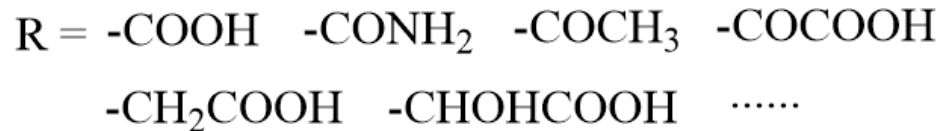
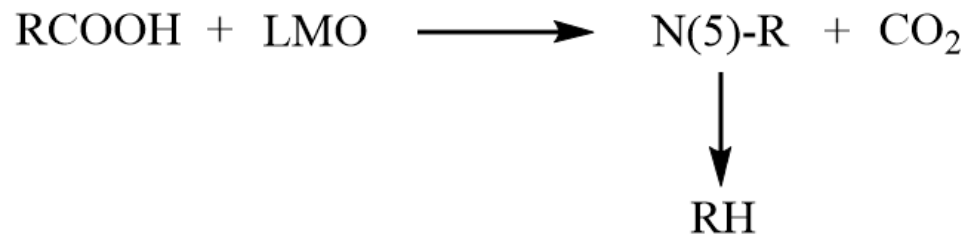
Lactate Monooxygenase (LMO)

Biological function:

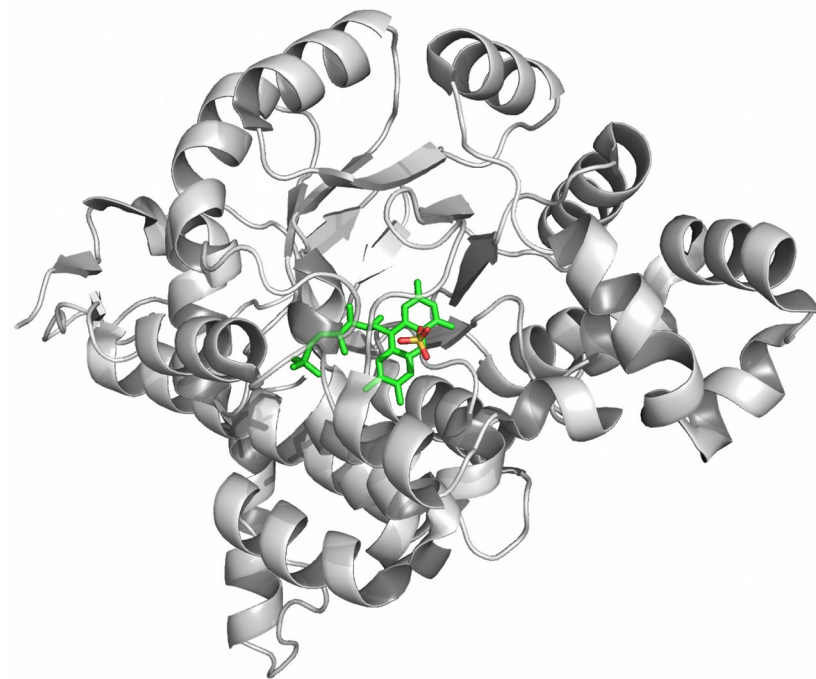


Lactate Monooxygenase (LMO)

Photoreaction:

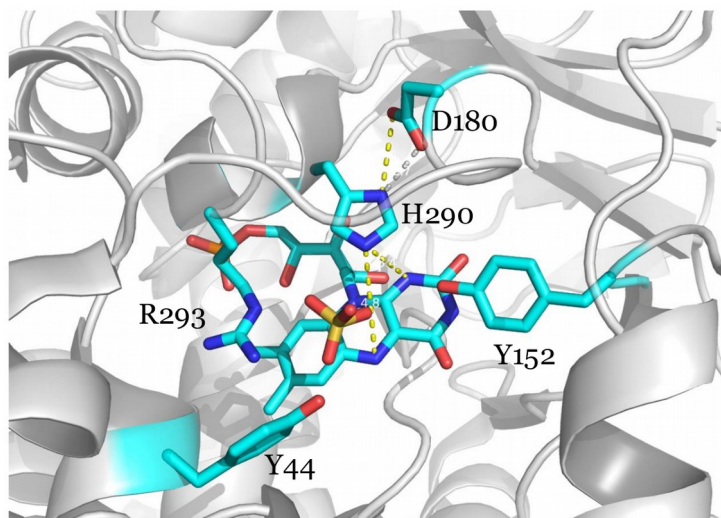


Mechanism?

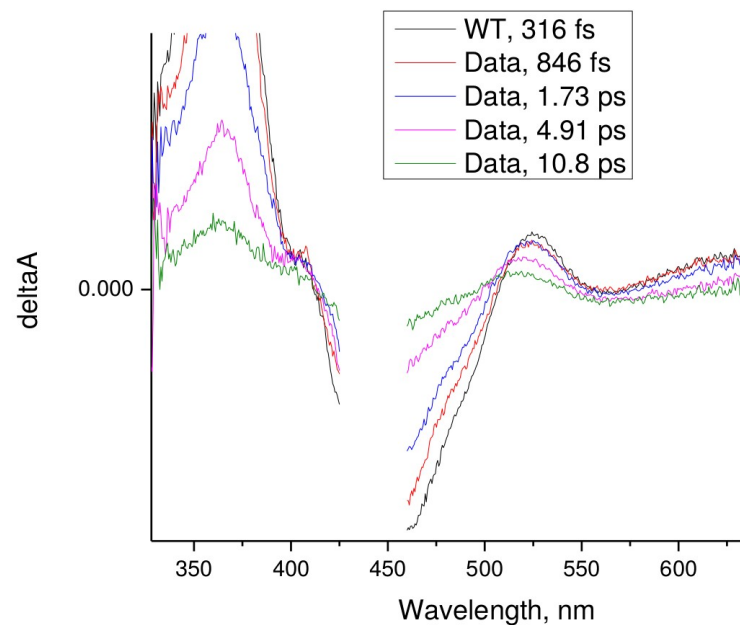


Experimental data

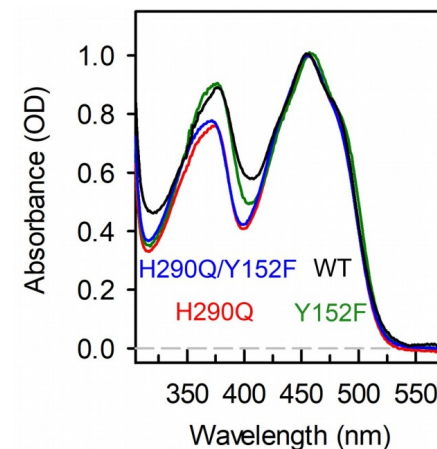
Intrinsic ET (apo state)



Pump-probe spectroscopy

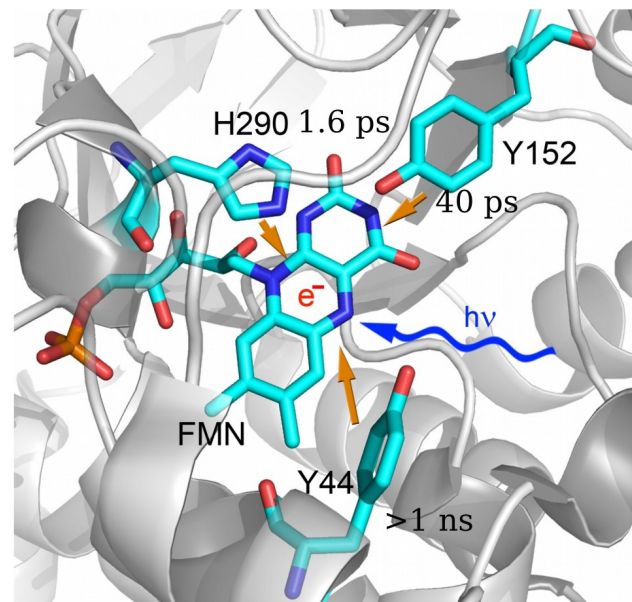
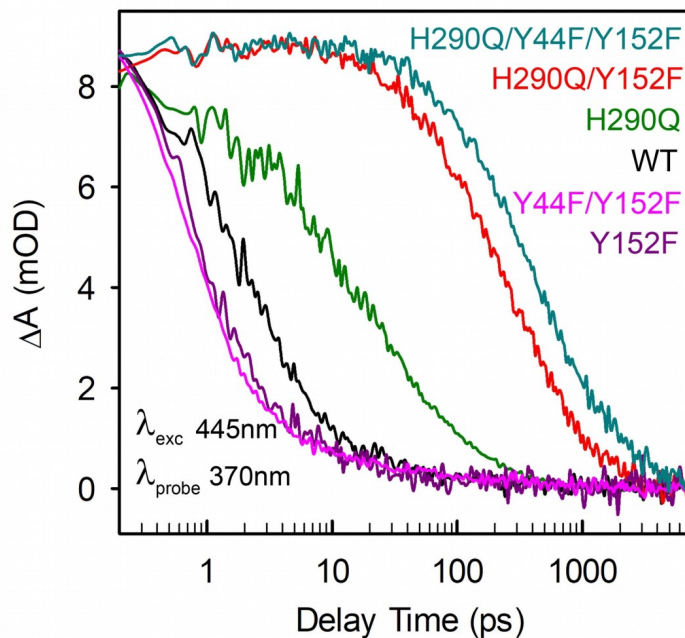


Pump @ 445 nm



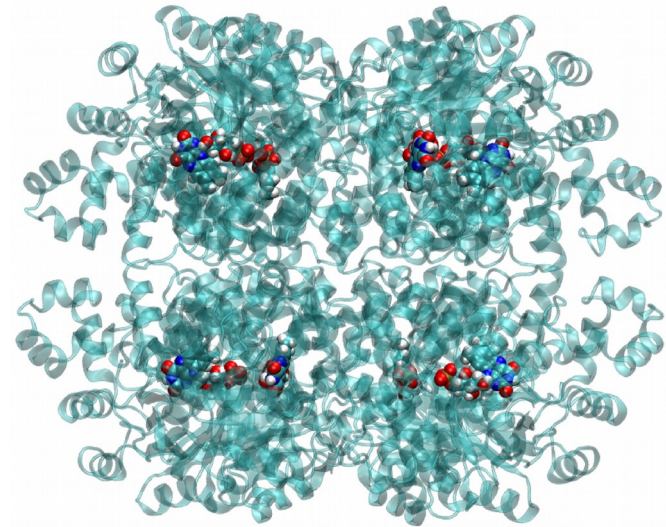
Experimental data

Intrinsic ET (apo state)



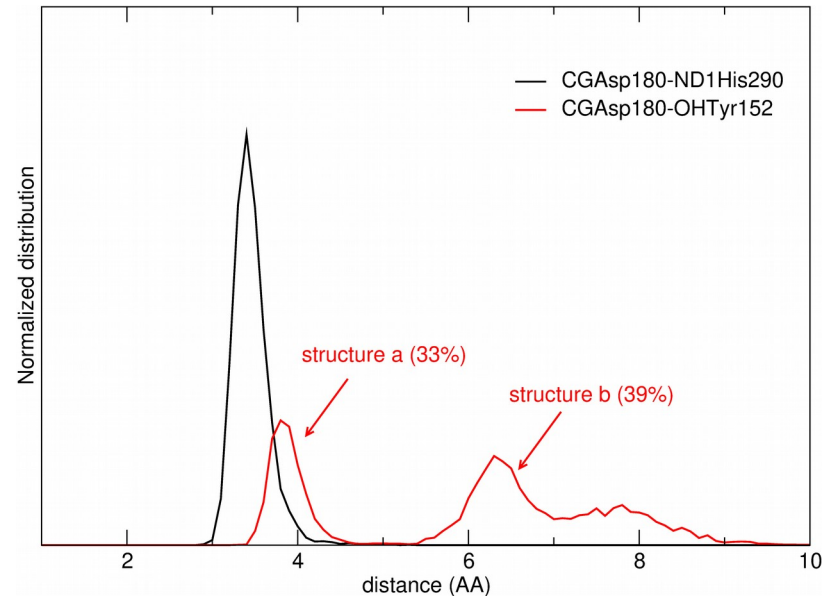
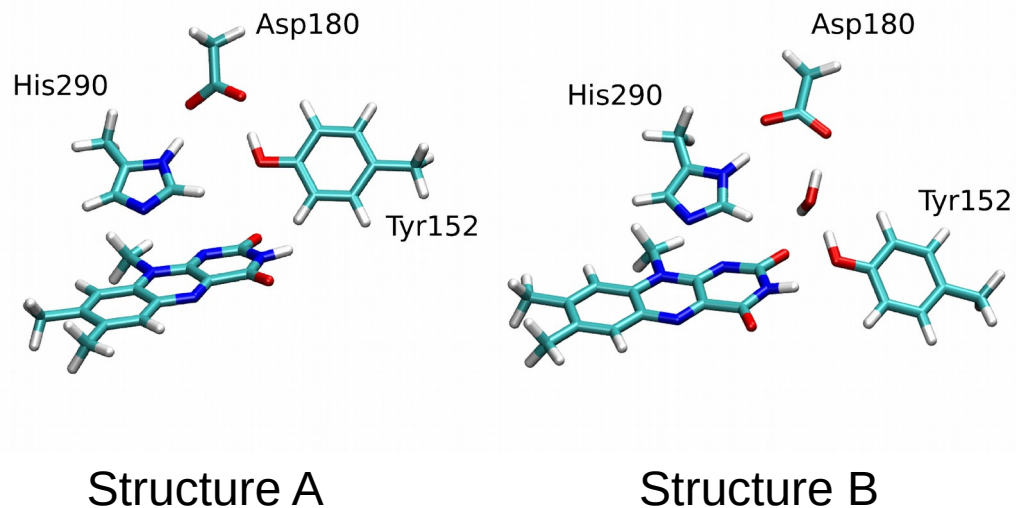
Computational data: intrinsic ET

75 ns-long MD simulation of
LMO octamer in solution
in the first excited state



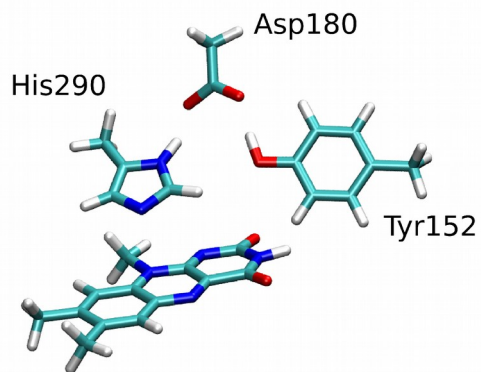
Computational data: intrinsic ET

75 ns-long MD simulation of LMO octamer in solution in the first excited state

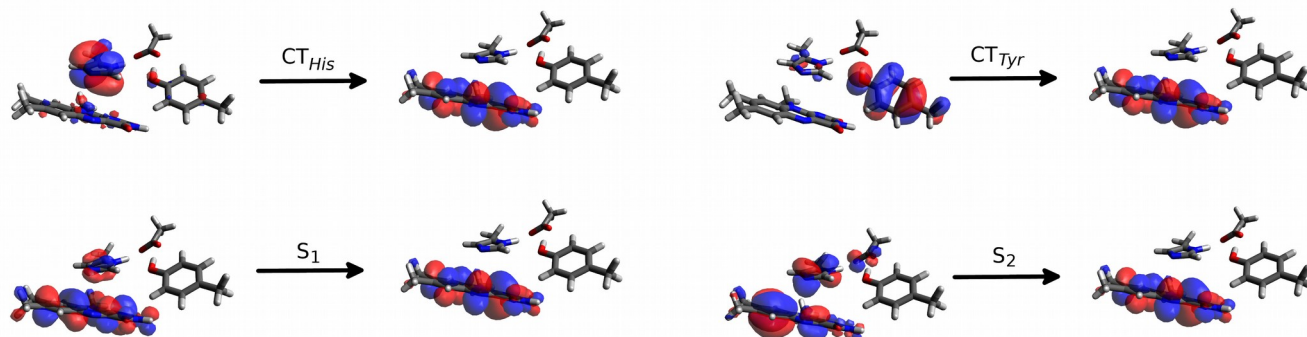


Computational data: intrinsic ET

Gas phase QM calculations on structure A

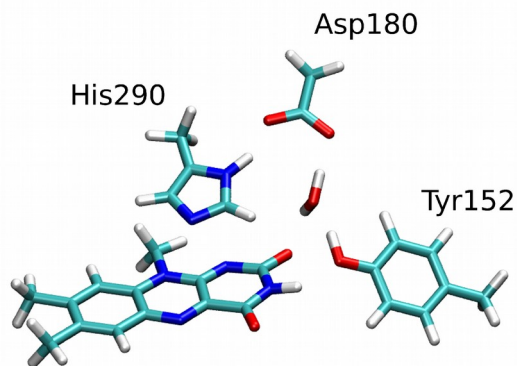


	Excitation Energy (eV)	Oscillator Strength
(1) CT_{His}	3.02	0.0090
(2) CT_{Tyr}	3.16	0.0006
(3) S_1	3.39	0.2861
(7) S_2	4.37	0.0843

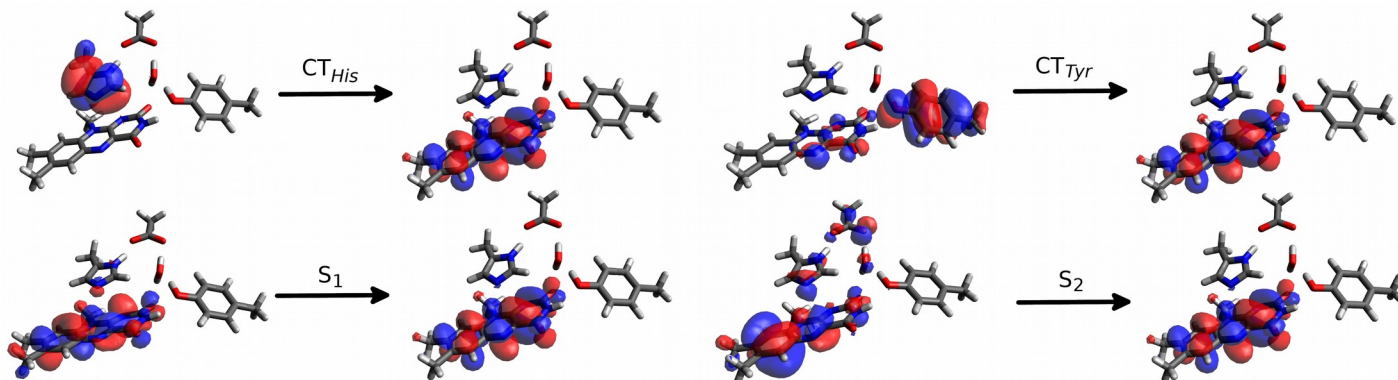


Computational data: intrinsic ET

Gas phase QM calculations on structure B

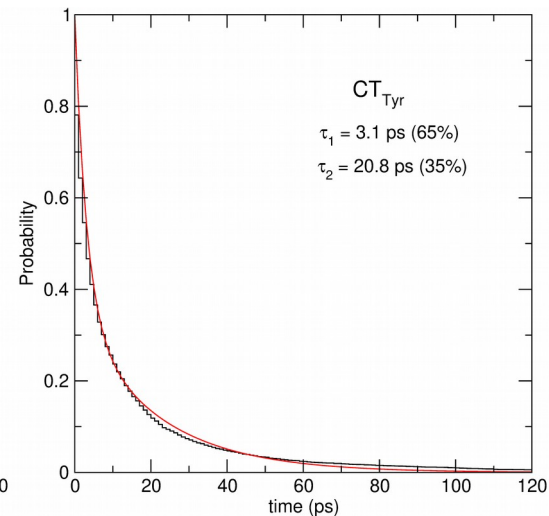
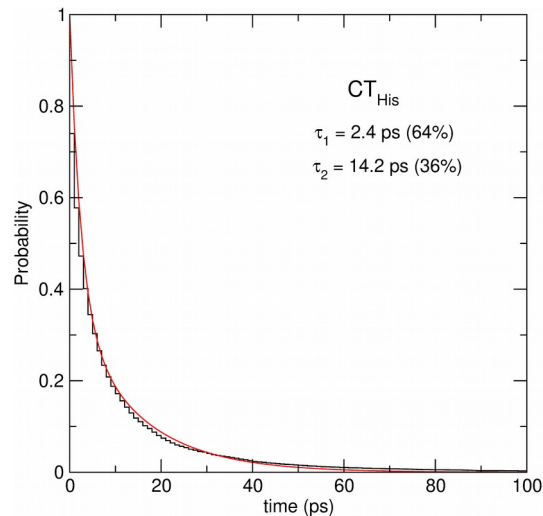
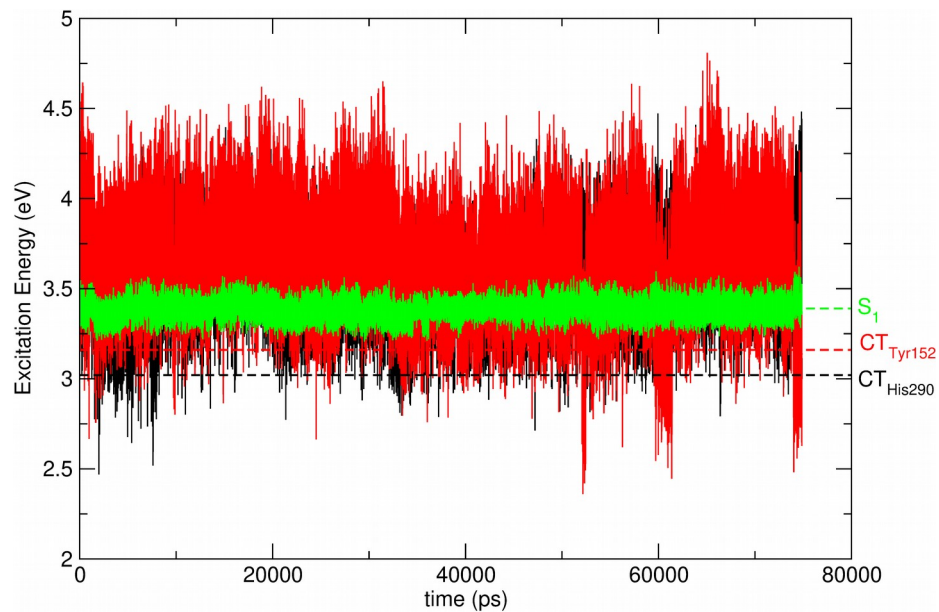


	Excitation Energy (eV)	Oscillator Strength
(1) CT_{His}	3.00	0.0035
(2) S_1	3.44	0.3163
(4) CT_{Tyr}	3.79	0.0005
(9) S_2	4.53	0.0684



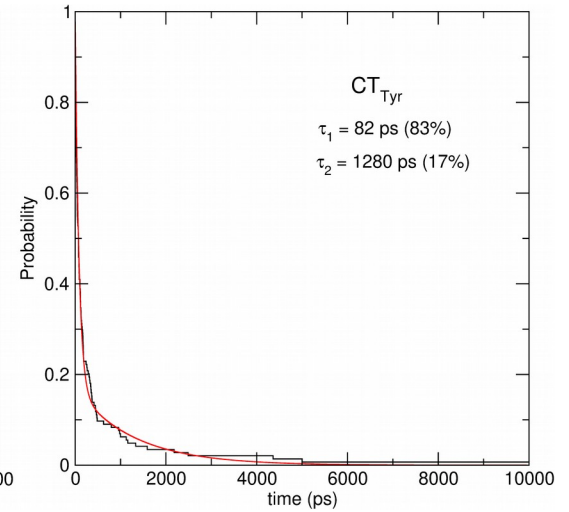
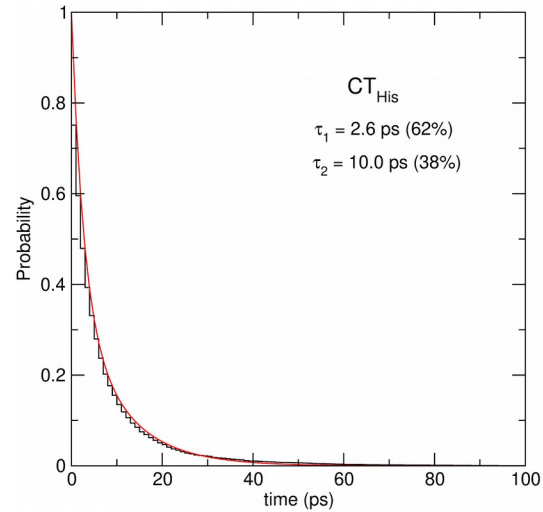
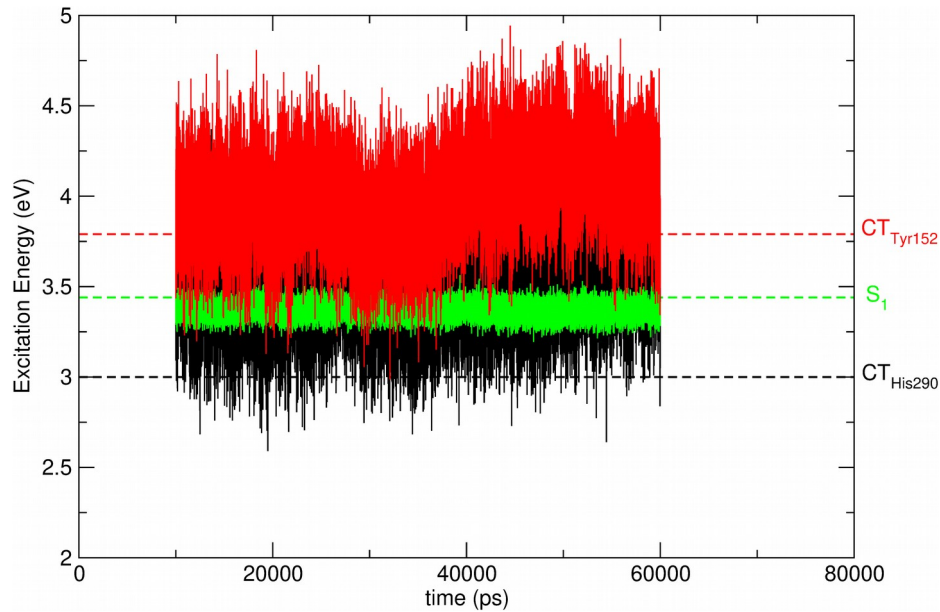
Computational data: intrinsic ET

Protein electrostatic effect inclusion for structure A



Computational data: intrinsic ET

Protein electrostatic effect inclusion for structure B

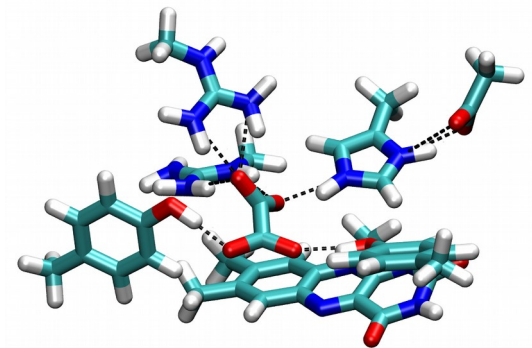
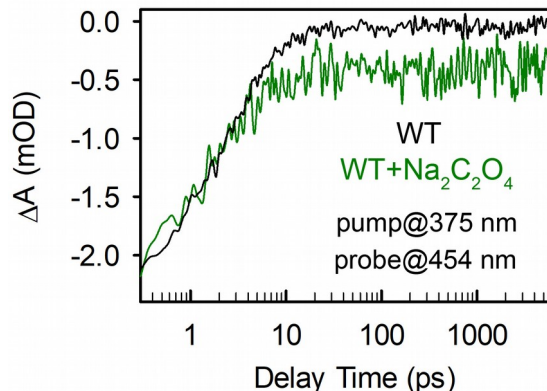


In summary

- **WT protein:** efficient ET from His290, less efficient ET from Tyr152. Subsequent PT from His/Tyr to Asp180
- **Y152F:** ET with His similar to WT but His/Asp PT more efficient as Tyr no longer competes
- **H290Q:** less efficient ET from Tyr152

Next:

Investigation of LMO
in complex with oxalate



Acknowledgments



Isabella Daidone



Jeremy C. Smith



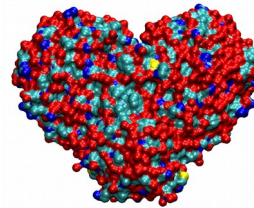
Chris Chipot



J.C. Gumbart



Xiankun Li
Gregory Scholes



Thank you
for your attention

